Temporal evolution of superradiance in a small sphere*

R. Friedberg and S. R. Hartmann
Columbia Radiation Laboratory, Department of Physics, Columbia University, New York, New York 10027
(Received 27 June 1974)

We discuss the problem of calculating the superradiant behavior in samples small compared to a radiation wavelength. Difficulties associated with the analysis of Dicke are considered in the framework of quantum electrodynamics and equivalently from a classical point of view. The evolution of superradiance in a small *sphere* is followed numerically with attention to spatial variation of the Bloch dipole density. Coherence is maintained except in the region $(kR)^{-1}|\cos\theta| \lesssim 2$ which is at the Bloch equator, where it suddenly disappears. Away from the equator, the spatial variations of dipole density oscillate with amplitude $\sim (kR)^2 \sin\theta$ and frequency $\sim (kR)^{-3}|\cos\theta|$. All these results agree with the predictions of a theoretical discussion previously published.

I. INTRODUCTION

Since the classic work of Dicke[1] the problem of superradiance has attracted considerable interest. Coherent spontaneous radiation of atoms cannot generally be treated as though the separate atoms radiate independently of each other. As pointed out by Dicke this simplified picture would overlook the fact that all atoms are interacting with a common radiation field. The method he chose was to treat the atom ensemble as a single quantum-mechanical system with energy states representing various degrees of correlation within the system. He began by treating a sample small compared to λ and then extended his work to large samples.

A. Large-sample problem

For samples large compared to a wavelength, the Dicke analysis of time evolution is complicated because from any given energy state there are a multitude of energy states to which one can proceed by spontaneous emission of radiation. This evolution from a single Dicke state to an ensemble of Dicke states can be understood from the elementary observation that light passing through an inverted medium is amplified and hence is spatially nonuniform along its direction of propagation. This complication has so far limited progress in understanding the evolution of large sample superradiance by a Dicke state analysis. Single-mode and phenomenological analyses of this process, which ignore this complication, abound but they are necessarily of limited use in predicting time-dependent behavior.[2,3] If, on the other hand, one attacks the long-rod problem semiclassically by a coupling of Maxwell's and Bloch's equations, the multimode character of the problem is readily handled and one obtains reasonable agreement with experiment.[4]

B. Small-sample problem

The small-sample problem has been considered relatively simple by Dicke and others because it has been thought permissible to replace $e^{i\vec{k}\cdot\vec{r}}$ by 1. It then follows that there is only one Dicke state to which a given Dicke state will radiate. The resulting simplicity makes this problem quite tractable and it has consequently been studied extensively.[5,6] This notion oversimplifies the problem, however, because it neglects the spatial variation of the electric field which arises not in the radiation component but in the near dipolar component of the field. (Quantum mechanically, the near field involves virtual photons of high momentum, for which the approximation $e^{i\vec{k}\cdot\vec{r}} \to 1$ must fail.)

We have recently argued that the major effect of these nonuniform fields is to induce spatially varying frequency shifts which render the superradiant state unstable.[7] However, for a small sphere to which we specialize herein, we have found the time evolution to be bizarre inasmuch as there are large regimes where it surprisingly follows Dicke's equation

$$\dot{\theta} = (I_0 r/\hbar\omega_0)\sin\theta \tag{1}$$

in spite of the effects of the nonuniform fields mentioned above. It is only near the equator of the Bloch sphere that superradiance in a small sphere changes abruptly to incoherence, and presumably the radiation then remains incoherent until all atoms are in their ground state.[8] (The angle θ is the tipping angle of the Bloch vector on the Bloch sphere. I_0 is the incoherent intensity, r is the cooperation number, and E is the energy separation of the Dicke states.)

In support of the findings noted above we propose to present a numerical analysis which we will describe in detail and whose results we will compare with the formulas of Ref. 8 which predict stability behavior and instability thresholds. But first we

will discuss to what extent superradiance in a small sample is understood and indicate the lack of any connection between Eq. (1) and any radiation-damping experiment of which we know.

II. SUPERRADIANCE: BASIC NOTIONS

A. What is superradiance?

According to Dicke "a gas which is radiating strongly because of coherence will be called superradiant."[1] This definition applies to states excited by the pulse technique commonly used in magnetic resonance, even though these states cannot be assigned a Dicke quantum number m. The so-called Dicke states (r, m) have (for large r) an abnormally large spontaneous emission rate, but as noted by Dicke[1] their stimulated emission rate is normal.[9] The NMR pulse technique, on the other hand, produces states whose spontaneous and stimulated emission rates are *both* abnormal; these states are described as a linear combination of Dicke states of fixed r with varying m, or by a Bloch vector with magnitude r and direction (θ, φ).

There is no essential difference between the Dicke state (r, m) when $m = r\cos\theta$ and the Bloch state (r, θ, φ) except that the phase of the precessing dipole moment in the latter case is known. The relation of this phase to that of an incident e-m field determines whether the stimulated process will be emission or absorption and how (abnormally) fast it will take place. For a Dicke state the phase of the dipole moment is not known, and stimulated emission and absorption are nearly equally likely. The average over many trials will be the normal stimulated emission rate (if the population is inverted) or the normal absorption rate (if it is not). This point enters into Planck's derivation[10] of the equilibrium partition of energy between a resonator and the field.

In other words, the dipole moment, which controls stimulated emission, has an expectation value $\sim r\sin\theta$ in the Bloch state but 0 in the Dicke state. In both cases, the expectation value of the square of the dipole moment, which controls spontaneous emission, is the same. Since we are concerned in this paper with spontaneous emission, we shall consider the term "superradiant" equally applicable to a Dicke state with $(r+m)(r-m+1) \gg \frac{1}{2}N+m$ and to a corresponding Bloch state.[11]

B. Superradiance with strong inhomogeneous broadening

When the inhomogeneous broadening is very large, the time development of superradiance is easily calculated. In fact, the dipole moment decays according to the Fourier transform of the line shape; this behavior is called free-induction decay. The origin of this decay is not in any change in the system's state due to radiation reaction, but in the loss of coherence through dephasing among atoms with different natural frequencies. The radiation is, to be sure, temporarily enhanced by coherence and therefore "superradiant," but it is not strong enough to deplete the system's energy by a significant fraction during the dephasing time T_2^*. Therefore one may just as well neglect radiation reaction in the calculation.[12] The condition for this approximation is roughly $T_s \gg T_2^*$, where T_s^{-1} is a measure of the atomic radiative decay rate as enhanced by superradiance.[13]

C. Superradiance with negligible inhomogeneous broadening

It is the opposite limit $T_s \ll T_2^*$ that chiefly concerns us here since in it the time development of the system is dominated by cooperative effects. Here we can consider the resonant atoms as truly identical and write the interaction Hamiltonian as

$$H = H_0 + \hbar\omega_0 \sum_{j=1}^{N} R_{3j} - \sum_{j=1}^{N} \vec{A}(\vec{r}_j)\cdot(\hat{\epsilon}_1 R_{1j} + \hat{\epsilon}_2 R_{2j}), \quad (2)$$

where ω_0 is the natural frequency including the single-atom Lamb shift; $\vec{r}_j$ is the position of the jth atom; and R_{1j}, R_{2j}, R_{3j} are the 2×2 matrices defined by Dicke.[1]

Dicke treated this Hamiltonian for a sample $\ll\lambda$ by two approximations. First, he replaced $\vec{A}(\vec{r}_j)$ by $\vec{A}(0)$ on the ground that the field does not vary much over a small fraction of a wavelength. Thus, he obtained

$$H = H_0 + \hbar\omega_0 \sum_{j=1}^{N} R_{3j} - \vec{A}(0)\cdot\sum_{j=1}^{N}(\hat{\epsilon}_1 R_{1j} + \hat{\epsilon}_2 R_{2j}). \quad (3)$$

Second, he considered only that part of the last term of Eq. (3) leading to real radiative transitions. This led to a transition rate proportional to

$$\left(\sum_j R_{1j}\right)^2 + \left(\sum_j R_{2j}\right)^2 = r(r+1) - m^2, \quad (4)$$

where $r(r+1)$, m are respectively the eigenvalues of $\sum_{\alpha=1}^{3}(\sum_j R_{\alpha j})^2, \sum_j R_{3j}$ for the initial state of the sample.

The crucial point in Dicke's analysis of the time behavior is that the Hamiltonian (3) commutes exactly with $\sum_{\alpha=1}^{3}(\sum R_{\alpha j})^2$, so that the quantum number r in (4) is a constant of the motion. The quantum number m decreases at a rate proportional to Eq. (4), so that if we take $\cos\theta \simeq m/r$ we arrive at Eq. (1). This equation is supposed to describe not only the initial rate of change of θ but its whole subsequent behavior, so that by integration one obtains

$$\cos\theta(t) = -\tanh[(I_0 r/\hbar\omega_0)(t - t_{90°})], \quad (5a)$$

or in terms of T_s [13]

$$\cos\theta(t) = -\tanh[(2/T_s)(t - t_{90°})]. \tag{5b}$$

It must be emphasized that the validity of Eqs. (5) depends on the constancy of r in time.

D. Critique of Dicke's second approximation

What has been omitted by Dicke's two approximations? If we continue to make the first one, leading to Eq. (3), and apply the Wigner-Weisskopf technique to the last term of Eq. (3), we obtain a self-interaction of the form

$$V = \left[\left(\sum_j R_{1j}\right)^2 + \left(\sum_j R_{2j}\right)^2\right] \int_{-\alpha}^{\alpha} \frac{f(\omega)}{\omega - \omega_0 + i\epsilon}\, d\omega, \tag{6}$$

where f need not be examined at present, but

$$\int_{-\alpha}^{\alpha} \frac{f(\omega)}{\omega - \omega_0 + i\epsilon}\, d\omega = P \int_{-\alpha}^{\alpha} \frac{f(\omega)}{\omega - \omega_0}\, d\omega + i\pi f(\omega_0). \tag{7}$$

In Dicke's treatment the first term of Eq. (7) is dropped, and the second term yields the decay rate given by Eqs. (5) and (1). But how large is the principal-part term?

As it stands, the integral in Eq. (7) diverges. However, Fain and others[5] have pointed out that it should be cut off at $\omega \sim c/a$, where a is a dimension of the sample, since coherence is lost at higher wave numbers. As $f(\omega) \sim \omega$ for $\omega \gg \omega_0$, this makes the first term of (7) *exceed* the second term by $O[\Lambda]$, where $\Lambda = \lambda_0/a \gg 1$.

This in itself is no catastrophe; it means only that the real part of (6), which Dicke's treatment ignores, causes a frequency shift[5] of order $(I_0 r/\hbar\omega_0)\Lambda \cos\theta$. The fact that this shift far exceeds the inverse lifetime of the system, and that it also varies with θ and hence with time, does not invalidate Dicke's equations for θ. A rapid azimuthal precession of the Bloch vector[14] is simply superimposed on the decay described by Eqs. (1) and (5).

At this point we should mention that the Hamiltonian (2) is incomplete and should be supplemented with a Coulomb interaction between dipoles. Equivalently,[15] we may take Eq. (2) as it is except that the interaction term is replaced by one involving not $\vec{A}$ but $\vec{E}_\perp$. The latter form is more convenient for making Dicke's first approximation; we replace $\vec{E}_\perp(\vec{r}_j)$ by $\vec{E}_\perp(0)$. The result is that f in Eq. (6) grows as ω^3 instead of as ω, so that after making the cutoff we find that the first term of Eq. (7) contains an additional part corresponding to the Coulomb interaction and yielding a frequency shift of order $(I_0 r/\hbar\omega_0)\Lambda^3 \cos\theta$. Such shifts have been discussed by Lorentz, Kittel, and others[16]; in a spherical sample, however, the Coulomb term vanishes.

At any rate, the Coulomb shift raises no new difficulties. The precession of the Bloch vector[14] just takes place faster when it is present. We conclude that Dicke's second approximation [dropping the first term of Eq. (7)] causes no serious error with respect to Eqs. (1) and (5), *provided* that one accepts his first approximation [replacement of Eq. (2) by (3)]. But this approximation is highly questionable.

E. Critique of Dicke's first approximation

Let us apply the Wigner-Weisskopf approach directly to Eq. (2), with the Coulomb term added. Instead of Eq. (6), we obtain (dropping the single-atom Lamb shift)

$$V = \sum_{j \neq j'} (R_{1j} R_{1j'} + R_{2j} R_{2j'}) V_{jj'}, \tag{8}$$

where $V_{jj'}$ depends strongly on the distance $r_{jj'} = |\vec{r}_j - \vec{r}_{j'}|$; in fact, $V_{jj'}$ is just the classical delayed dipole-dipole interaction, also called the Stephen potential.[17] Its real part consists of the Coulomb interaction $\sim 1/r_{jj'}^3$, plus a correction whose leading term is $\sim 1/r_{jj'}$. Its imaginary part is constant for distances $\ll \lambda_0$.

It is evident, then that the replacement of Eq. (2) by (3) is valid only as far as the imaginary part of $V_{jj'}$ is concerned, and not the real part. Another way to say this is that the Fain cutoff should be taken at $\omega \sim c/r_{jj'}$ rather than $\omega \sim c/a$, so that the principal part of the integral in Eq. (6) really depends on which term of the expansion of $(\sum R_{1j})^2$ or $(\sum R_{2j})^2$ one is considering. Or again, the replacement $\vec{A}(\vec{r}_j) \to \vec{A}(0)$ depends on the smallness of the sample compared to wavelength, yet the first term of Eq. (7) is dominated by short wavelengths $\ll \lambda_0$ (very high-momentum virtual photons) for which this condition is not satisfied.

We now see that the replacement of Eq. (2) by (3) omitted a serious complication. The atomic operators $\sum_j R_{1j}$ and $\sum R_{2j}$ in Eq. (3) commute with $\sum_{a=1}^{3} (\sum R_{aj})^2$, and consequently Dicke's r appears as a constant of the motion in any treatment based on Eq. (3). But the Hamiltonian (2) does not have this property. Accordingly, V as given by Eq. (8), as opposed to (6), fails to commute with $\sum_{a=1}^{3} (\sum R_{aj})^2$ because of the variations of $V_{jj'}$. Therefore if the real part of $V_{jj'}$ is retained and its dependence on $r_{jj'}$ is respected, Dicke's r is no longer a constant of the motion.

An alternative statement of the same difficulty begins with the observation that the real part of the electric field (that part in phase with the collective dipole moment) gives rise to a frequency

shift. Since the strength of this real field varies throughout the sample, coherence between parts of the sample is lost in a time inverse to the variation of the shift; but this time is much too short for appreciable damping to take place according to Eq. (5), because the real field varies by an amount far exceeding the imaginary (damping) field.

Dicke's original intention may have been to absorb the short-range part of $V_{jj'}$ into H_0. This would be permissible if the interaction were *very* short-range ($\sim 1/r_{jj'}^4$, or faster as $r_{jj'} \to \infty$) since then it could be claimed that all atoms, except a small fraction near the surface, have similar neighborhoods and therefore feel nearly the same total field. That is, $\sum_{j'} V_{jj'} R_{1j'}$ would then be nearly independent of j, if $R_{1j'}$ were assumed independent of j'. But the terms in $1/r_{jj'}^3$ and $1/r_{jj'}$ fall off too slowly to be treated in this way, and yet too quickly to be taken as constant.

F. NMR with high-Q coil

The above objection may be greeted with some skepticism because behavior resembling Eq. (5) has actually been observed in small-sample NMR experiment.[18] However, it must be stressed that such experiments are not performed on a sample radiating into free space. They contain an additional element, a high-Q coil surrounding the sample and tuned to the frequency ω_0. Under these conditions the deexcitation of the sample is not caused by its own radiation field but by the quasistatic field of the coil. In fact, the whole process involves no radiation at all but merely nonradiative transfer of energy from the sample to the coil, where the energy is dissipated ohmically.

It may be instructive to examine the formula[19]

$$d\theta/dt = 2\pi Q\gamma M_0 \sin\theta \tag{9}$$

describing this process. Superficially, it resembles Eq. (1). However, the quantity γM_0 (γ is the gyromagnetic ratio, M_0 is the magnetization density) is of order $\Lambda^3 I_0 \gamma/\hbar\omega_0$, so that the decay proceeds $\sim\Lambda^3 Q$ times faster than in the process studied by Dicke. The factor Λ^3 arises from the nonradiative nature of the process; it is the real (quasistatic) field of the sample that excites the coil, not the much smaller imaginary (radiative) field. This is quite evident in the derivation[19] of Eq. (9).

The tuned coil does three things to the quasistatic signal it receives from the sample: it amplifies it by Q, retards it by 90°, and throws it back to the sample. Thus, the sample feels a damping field $\sim\Lambda^3 Q$ times its own radiation field. Since the nonuniform frequency shifts that should lead to loss of coherence are of order $\Lambda^3 T_s^{-1}$, whereas the enhanced damping rate is of order $\Lambda^3 Q T_s^{-1}$, coherence is maintained during the damping process. (It is, of course, also necessary that $\Lambda^3 Q T_s^{-1} \gg T_2^{*-1}$; this was the original purpose of the high Q.)

Behavior similar to Eq. (5) could also be obtained, in principle, by placing the sample in a tuned cavity with enormous Q ($\gg\Lambda^3$). The process would then be radiative and the enhanced damping rate would then be $\sim Q T_s^{-1}$ instead of $\Lambda^3 Q T_s^{-1}$. However, the damping field would have the cavity walls as its source, and not the sample.

We may sum up by saying that a sample may indeed be made to follow a modification of Eq. (5) with enhanced damping rate $\gg\Lambda^3 T_s^{-1}$ by placing it in a tuned (here necessarily reflecting) cavity or tuned coil; but this fact does not mean that coherence is not lost in the manner described in Sec. II E, only that the enhanced damping rate is sufficient to outrace the dephasing. The NMR experiments do nothing to show that Eq. (5) would correctly describe radiation into free space, for which the damping rate is not enhanced by any external element.

III. SMALL SPHERE

A. Shape dependence

Because of the tensor nature of the dipolar interaction, the field-induced dephasing effects are highly geometry dependent. There are, in fact, pathological cases where the dephasing effects are missing. This occurs when the symmetry is such that each atom sees exactly the same field and is exemplified by a ring of atoms ordered in single file. Two interacting dipoles are just a special case of this configuration.

Aside from these pathological cases it is worthwhile distinguishing between those shapes called regular, in which the electrostatic field due to a uniform density is uniform or nearly so (any approximately ellipsoidal shape) and all other (i.e., most) shapes, which we call irregular. The regular shapes are the most stable, because the dephasing rate is only $\sim\Lambda T_s^{-1}$ instead of $\Lambda^3 T_s^{-1}$.

B. Superradiant line shapes

A relative measure of the importance of two processes can be obtained from a comparison of the linewidth they give rise to. For incoherent spontaneous emission the linewidth is Lorentzian and given by the formula

$$g(\omega) = (1/\pi)\, T_1^{-1}/[(\omega - \omega_0)^2 + T_1^{-2}], \tag{10}$$

where T_1 is the lifetime. (T_1^{-1} is the half-width at half-maximum.) This is to be compared with the Fourier transform of the free decay of N atoms

in a volume $\ll \lambda$ after excitation by a $\frac{1}{2}\pi$ pulse as calculated by Dicke,

$$a(\omega) = \tfrac{1}{2}\pi(1/\alpha)\,\mathrm{sech}[\tfrac{1}{2}\pi(\omega-\omega_0)/\alpha], \tag{11}$$

$$\alpha = (I_0/\hbar\omega_0)(\tfrac{1}{2}N), \tag{12}$$

which has a full width at half-maximum of

$$\Delta\omega = \frac{1.12}{2}\,\frac{I_0}{\hbar\omega_0}\,\frac{N}{2}, \tag{13}$$

and since $I_0/\hbar\omega_0 = T_1^{-1}$ it is a factor of $O(N)$ larger than the incoherent width. But the frequency distribution induced by the spatially varying real field from a uniform polarization is even wider since the spatially varying local frequency shift in a small sphere has been calculated to be[7,20]

$$\Delta\omega = \tfrac{3}{4}NT_1^{-1}(kR)^{-1}\{1-\tfrac{1}{5}(r/R)^2[2-(\hat{P}_0\cdot\hat{r})^2]\}\cos\theta, \tag{14}$$

which yields a frequency distribution given by

$$\rho(\omega) = \frac{3}{4\beta^{3/2}}\,(\beta - |\omega_0-\beta-\omega|)^{1/2} \quad \text{for } \omega_0-2\beta<\omega<\omega_0 \tag{15}$$

and $\rho(\omega)=0$ otherwise. The quantity β is $\frac{3}{20}(N/T_1)\times(kR)^{-1}/|\cos\theta|^{-1}$. The rms second moment is

$$(\Delta\omega^2)^{1/2} = \tfrac{3}{5}(\tfrac{8}{35})^{1/2}(N/4T_1)(kR)^{-1}\cos\theta. \tag{16}$$

This distribution is a factor $(kR)^{-1}$ wider than the Dicke shape and consequently cannot be neglected.

A comparison of these line shapes is given in Fig. 1 for a sphere of 20 atoms spaced so that $(kR)^{-1}=15$.

C. Stability in regular shapes

The frequency distribution given in Eq. (15) and in Fig. 1 refers only to the initial time, when the polarization density is uniform throughout the sample. As parts of the sample dephase under the nonuniform shift (14), the polarization density $\vec{P}(\vec{r})$ becomes nonuniform and the field it produces is altered. A little thought shows that when the fractional variation of $\vec{P}$ is as large as Λ^{-2}, the Coulomb field due to variations of $\vec{P}$ is of the same order as the field giving rise to Eq. (14). [This is true only of regular samples, in which Eq. (14) receives no Coulomb contribution and is thereby reduced by Λ^2.]

It follows that all we have said so far in the present paper and in Ref. 7 is insufficient to determine whether Eq. (5) is valid for regular samples. We have shown only that the initial rate of dephasing is such that, *if it continues*, coherence will be lost in a time $\sim\Lambda^{-1}T_s$. But does it continue? That question can be answered only by studying the nonuniform Coulomb field produced by the nonuniform polarization density produced by Eq. (14).

D. Predictions for the sphere

In a recent paper[8] we carried out such an analysis and predicted that small samples of regular shape would follow Dicke's equation (5) to some extent in spite of the fact that the dispersion in the real field exceeds the imaginary field by $O[\Lambda\cos\theta]$. For the sphere, with atoms feeling a local field $\vec{E}+\frac{4}{3}\pi\vec{P}$, the following predictions were made:

(i) If all atoms begin in the same state, corresponding to a Bloch vector reasonably far below the equator ($\theta>\frac{1}{2}\pi$) the decay will follow Dicke's equation down to the ground state.

(ii) Under the conditions of (i) but with initial $\theta<\frac{1}{2}\pi$, the decay will follow Dicke's equation down to the vicinity of the equator.

(iii) Under the conditions of (i) and (ii) the Bloch vectors of different parts of the sample will remain *nearly* equal, but their small differences will oscillate with transverse amplitude $\sim\Lambda^{-2}\sin\theta$ and with a mixture of periods $\sim T_s\Lambda^{-3}|\sec\theta|$.

(iv) If the initial Bloch vector is sufficiently close to the equator, $|\cos\theta|\lesssim\Lambda^{-1}$, the system will remain coherent for a time $T_\Delta\sim T_s\Lambda^{-2}$ after which the local Bloch vectors will suddenly (in a further time

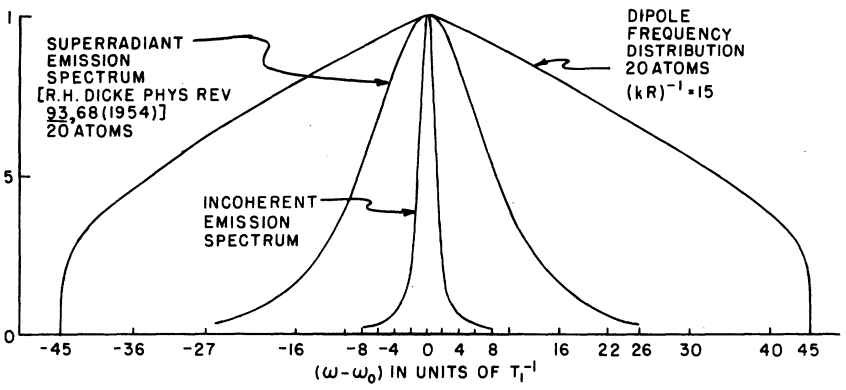

FIG. 1. Normalized line shape plotted as a function of $(\omega-\omega_0)$ in units of T_1^{-1} for (a) incoherent spontaneous emission, (b) superradiant emission of 20 atoms assuming that coherence is maintained throughout the decay, (c) 20 atoms with $(kR)^{-1}=15$, taking the initial position-dependent shifts into account with the Bloch vector near the north pole.

$\sim T_s\Lambda^{-3}$) develop large spatial variation and the radiated intensity will drop to the incoherent rate.

(v) Under the conditions of (iv) the relation between T_Δ and θ can be written $\Lambda^2 T_\Delta/T_s = f(\Lambda|\cos\theta|)$, where f is a universal function (independent of Λ) for which an expression was given.

(vi) If the initial θ has $|\Lambda^{-1}| \lesssim |\cos\theta| \lesssim 1/\ln|\Lambda|$, dephasing should occur as in (iv) but after a delay T_Δ somewhere between $T_s\Lambda^{-2}$ and T_s. This prediction was less certain than the others.

In view of the bizarre appearance of some of these predictions and the unfamiliarity of the analysis that led to them, we have checked them against a straightforward computer calculation in which *no account was taken, a priori,* of the conceptual methods of Ref. 8—in particular, of the electrostatic modes described there. Our results have fully confirmed predictions (i)–(iv) and agree quite closely with prediction (v). Further computation at large values of $(kR)^{-1}$ will be required to check prediction (vi).

IV. NUMERICAL COMPUTATION: METHOD

A. Ideal system

The system we studied has ideally the following physics. A sphere of radius R is alone in free space. The matter within the sphere is described by a local Bloch vector $\vec{p}(x,y,z,t)$ where x,y,z are the coordinates of an arbitrary point and t is the time. The first two components of $\vec{p}$ in Bloch space determine a complex polarization density

$$P(x,y,z,t) = P_0[p_1(x,y,z,t) - ip_2(x,y,z,t)], \tag{17}$$

which is taken to be in the z direction in real space. The electric field (E_x, E_y, E_z) is determined as a function of x,y,z,t by Maxwell's equations in the form (henceforth we write k rather than k_0 for the wave number of resonant light)

$$\begin{aligned} &\frac{\partial E_x}{\partial x} + \frac{\partial E_y}{\partial y} + \frac{\partial E_z}{\partial z} = -4\pi\frac{\partial P}{\partial z}, \\ &(\nabla^2 + k^2)E_x = 0, \quad (\nabla^2 + k^2)E_y = 0, \\ &(\nabla^2 + k^2)E_z = -4\pi k^2 P, \end{aligned} \tag{18}$$

with outgoing boundary conditions at infinity. (P is zero outside the sphere.) The local Bloch vector develops in time according to Bloch's equation

$$\frac{\partial}{\partial t}\vec{p}(x,y,z,t) = \gamma\vec{p}(x,y,z,t)\times\vec{\mathcal{E}}(x,y,z,t), \tag{19}$$

where

$$\mathcal{E}_1 - i\mathcal{E}_2 = E_z + \tfrac{4}{3}\pi P, \quad \mathcal{E}_3 = 0. \tag{20}$$

The behavior of the system is completely determined by Eqs. (17)–(20), if $\vec{p}$ is given everywhere at $t=0$. Since the magnitude of $\vec{p}$ is time independent by Eq. (19), we take it to be unity at all points. The constants γ and P_0 enter the behavior of $\vec{p}$ only through their product γP_0, which should be identified with $(9/16\pi)(kR)^{-3}NT_1^{-1} = (9/4\pi)(kR)^{-3}T_s$ for comparison with Dicke's equation. [This identification depends on the fact that a uniform polarization density P_0 would produce a damping field $\frac{2}{3}ik^3(\frac{4}{3}\pi R^3)P_0$, to leading order in kR.]

The steps by which one passes from a realistic situation to the ideal system described above are generally familiar. We have neglected all but two atomic levels; we have replaced a discrete set of N atoms by a continuum; we have ignored the x and y components of the dipole moment operator; we have used $E + \frac{4}{3}\pi P$ as the local field; we have neglected the incoherent linewidth in comparison to T_s^{-1}; we have passed to the "rotating coordinate system" in Bloch space; we have neglected γP_0 in comparison to kc, the natural frequency. The limits of validity of these steps do not concern us here. We address ourselves only to the question, whether if we set $kR \ll 1$ this ideal system will follow the prediction of Ref. 8.

B. Removing the Coulomb singularity

In submitting this question to computer analysis, our intended strategy was as follows. Equations (18) do not involve time derivatives and therefore admit a solution in terms of a retarded spatial Green's function

$$E_z(x,y,z,t) = \int G(x,y,z;x',y',z') \times P(x',y',z',t)\,dx'\,dy'\,dz', \tag{21}$$

where the integration need not be carried outside the sphere since P vanishes there. We intended to divide the sphere into M small regions, where M would be as large as practicable. Within each (the ith) region we would choose a representative point (x_i, y_i, z_i). The various quantities $\vec{p}, P, \mathcal{E}, E_z$ would be evaluated only at these points. The basic approximation would be the replacement of the integral in Eq. (21) by a sum

$$E_z(x_i,y_i,z_i,t) \cong \sum_j \Omega_j G(x_i,y_i,z_i;x_j,y_j,z_j) \times P(x_j,y_j,z_j,t), \tag{22}$$

where Ω_j is the volume of the jth region.

This strategy, however, runs into a difficulty that turns on the question, whether Eq. (22) should include a term with $j=i$. The trouble is that G contains the $1/r^3$ singularity of the electrostatic dipolar field. Hence the integral in (21) is not absolutely convergent. It can, of course, be made

to converge by matching the contributions from dipoles located near but in different directions from the field point. However, the resulting convergent integral receives a contribution from the region $j=i$ that depends strongly on the shape of the region and *remains finite* when the size of the region is shrunk indefinitely. Therefore a substantial error is made in (22) if the term with $j=i$ is excluded; but the correct evaluation of this term would require a separate and awkward calculation.

To evade the difficulty, we modified our strategy by writing

$$P(x',y',z',t)=P(x,y,z,t)+[P(x',y',z',t) -P(x,y,z,t)]. \quad (23)$$

If this decomposition is applied to the right side of (21), we obtain two terms. In the first term $P(x',y',z',t)$ is replaced by $P(x,y,z,t)$, which can be taken outside the integral. This term can be evaluated analytically by solving Eqs. (18) for E_z in the case of uniform P. In the second term, the singularity in G is partially cancelled by the vanishing of $[P(x',y',z',t)-P(x,y,z,t)]$ as the two points coalesce. This term can be computed numerically by turning it into a sum analogous to (22); the error in omitting a term $j=i$ is now small when M is large, because the singularity has been weakened.

By solving Eqs. (18) with P uniform throughout the sample, we obtain[7]

$$\int G(x,y,z;x',y',z')\,dx'\,dy'\,dz' = F(x,y,z) = -\tfrac{4}{3}\pi+\tfrac{4}{3}\pi(kR)^2[1-\tfrac{1}{5}(\zeta^2+2\sigma^2)]+\tfrac{3}{9}i\pi(kR)^3+O((kR)^4), \quad (24)$$

where

$$\sigma^2=(x^2+y^2)/R^2, \quad \zeta^2=z^2/R^2. \quad (25)$$

Using this formula for the first term discussed above, and replacing the integral by a sum in the second term, we obtain instead of (22)

$$E_z^{(i)} \cong F_i P^{(i)}+\sum_{j\neq 1}\Omega_j G_{ij}(P^{(j)}-P^{(i)}), \quad (26)$$

where we have simplified the notation by writing F_i for $F(x_i,y_i,z_i)$, $P^{(i)}$ for $P(x_i,y_i,z_i,t)$, etc.

C. Annular regions

The number of regions required for a given accuracy is greatly reduced by the azimuthal symmetry of the ideal system. Supposing that at $t=0$ the function $\vec{p}$ depends on x,y,z only through the variables σ,ζ, the same will remain true of the exact solution to Eqs. (17)–(20) at all later times. Therefore, we can make each region a thin ring centered on the z axis, so that its extent is small in the σ and ζ directions but ranges from 0 to 2π in the representative circle, the locus of equations $\sigma=\sigma_i$, $\zeta=\zeta_i$. Equation (26) is still a good approximation, but G_{ij} must now be defined as an average over the representative circle in the jth region. That is,

$$G_{ij}=\frac{1}{2\pi}\int_0^{2\pi} G(R\sigma_i,0,R\zeta_i;R\sigma_j\cos\chi,R\sigma_j\sin\chi,R\zeta_j)\,d\chi. \quad (27)$$

If we substitute Eq. (27) into (26), using the customary expansion for the retarded Green's function

$$G(x_1,y_1,z_1;x_2,y_2,z_2)=(3z_{12}^2-r_{12}^2)/r_{12}^5+(z_{12}^2+r_{12}^2)k^2/2r_{12}^3+\tfrac{2}{3}ik^3+O[k^4r_{12}], \quad (28)$$

where $z_{12}=z_1-z_2$, $r_{12}^2=(x_1-x_2)^2+(y_1-y_2)^2+(z_1-z_2)^2$ and use the result in (24), we obtain

$$\begin{aligned}\frac{\mathcal{E}_1^{(i)}}{P_0}&\simeq(kR)^2[1-\tfrac{1}{5}(\zeta^2+2\sigma^2)]p_1^{(i)}+\sum_{j\neq i}R^{-3}\Omega_j[g_{ij}+(kR)^2h_{ij}](p_1^{(j)}-p_1^{(i)})+\tfrac{2}{3}(kR)^3\sum_{j\neq 1}R^{-3}\Omega_j p_2^{(j)},\\ \frac{\mathcal{E}_2^{(i)}}{P_0}&\simeq(kR)^2[1-\tfrac{1}{5}(\zeta^2+2\sigma^2)]p_2^{(i)}+\sum_{j\neq i}R^{-3}\Omega_j[g_{ij}+(kR)^2h_{ij}](p_2^{(j)}-p_2^{(i)})-\tfrac{2}{3}(kR)^3\sum_{j\neq i}R^{-3}\Omega_j p_1^{(j)},\end{aligned} \quad (29)$$

where if we write $\zeta_{ij}=\zeta_i-\zeta_j$, $\alpha_{ij}=\sigma_i^2+\sigma_j^2$, $\beta_{ij}=2\sigma_i\sigma_j$, we have

$$\begin{aligned}g_{ij}&=\frac{1}{2\pi}\int_0^{2\pi}\frac{2\zeta_{ij}^2-\alpha_{ij}-\beta_{ij}\cos\chi}{(\zeta_{ij}^2+\alpha_{ij}+\beta_{ij}\cos\chi)^{5/2}}\,d\chi,\\ h_{ij}&=\frac{1}{2\pi}\int_0^{2\pi}\frac{2\zeta_{ij}^2+\alpha_{ij}+\beta_{ij}\cos\chi}{2(\zeta_{ij}^2+\alpha_{ij}+\beta_{ij}\cos\chi)^{3/2}}\,d\chi.\end{aligned} \quad (30)$$

The equations actually submitted to the computer were only (19), (29), and (30). We began by choosing a number μ, considerably smaller than 1, to determine the region thickness. We enumerated all pairs (σ_i, ζ_i) for which

$$\sigma_i/\mu = \text{odd positive integer},$$

$$\zeta_i/\mu = \text{even integer (positive, negative, or zero)}$$

$$\sigma_i^2 + \zeta_i^2 \leq 1. \tag{31}$$

The ith region consisted of all points for which

$$|\sigma - \sigma_i| < \mu, \quad |\zeta - \zeta_i| < \mu \tag{32}$$

and its volume was

$$\Omega_i = 8\pi\mu^2\sigma_j R^3. \tag{33}$$

The numbers g_{ij} and h_{ij} were evaluated from (30) for each pair of regions, with the aid of fast subroutines for complete elliptic integrals of the first and second kinds. (All the above procedures were carried out by the program at the start of each run.) An initial tipping angle θ was then chosen, and all the $\vec{p}^{(i)}$ were set equal at $t=0$ with

$$p_1^{(i)} = \sin\theta, \quad p_2^{(i)} = 0, \quad p_3^{(i)} = \cos\theta. \tag{34}$$

The subsequent behavior of the $\vec{p}$'s was then followed by means of Eqs. (19) and (29) with the small number kR chosen in advance and the numbers $R^{-3}\Omega_j$; determined by (33).

We should make two remarks about (29). The first is that we have neglected $O[(kR)^4]$ or higher on the right-hand side—see Eqs. (24) and (28). We reason that the neglected fields are much smaller than the coherent damping field [the last term of Eq. (29)] and that they cannot therefore exert a significant effect within the coherent radiation lifetime $O[T_s] = O[P_0\gamma(kR)^3]$.

The second remark is that the leading term of (24) has cancelled the term $\frac{4}{3}\pi P$ in (20). Consequently, the electric field is not larger than $O[P_0(kR)^2]$, as long as the differences among the $\vec{p}^{(i)}$ are only $O[(kR)^2]$. In other words, we have let our program "know" *a priori* that the local field in a uniformly polarized sphere vanishes in the electrostatic approximation. This property of the sphere, which is essential to the predictions of Ref. 8, has been built into our computation exactly and will not be disturbed by any of our approximations—for example, by the fact that the regions defined by (33) and (34) do not constitute precisely a spherical volume. We emphasize, however, that our program does *not* "know" anything about the electrostatic modes of excitation, which play a major role in Ref. 8.

D. Steps in time

In following Eqs. (19) and (29) through time, we took care not to use any approximation that would violate the equation

$$\frac{\partial}{\partial t}|\vec{p}| = 0 \tag{35}$$

which is a consequence of Eq. (19). In simplest form, our method was as follows. A small number ν was chosen in advance, and each step in the calculation covered an interval of duration

$$\Delta t = \nu(P_0\gamma)^{-1}. \tag{36}$$

Letting t_0 be the value of t at the start of the interval, and supposing all the $\vec{p}^{(i)}(t_0)$ to be given, the program calculated all the $\vec{\mathcal{E}}^{(i)}(t_0)$ from Eq. (29). The incremented Bloch vectors $\vec{p}^{(i)}(t_0+\Delta t)$ were then evaluated as

$$\begin{aligned}\vec{p}^{(i)}(t_0+\Delta t) \cong\ & \hat{\epsilon}^{(i)}\cdot\vec{p}^{(i)}(t_0)\hat{\epsilon}^{(i)} \\ & + [\hat{\epsilon}^{(i)}\times\vec{p}^{(i)}(t_0)]\times\hat{\epsilon}^{(i)}\cos|\epsilon^{(i)}| \\ & + \vec{p}^{(i)}\times\hat{\epsilon}^{(i)}\sin|\epsilon^{(i)}|,\end{aligned} \tag{37}$$

where

$$\vec{\epsilon}^{(i)} = |\epsilon^{(i)}|\hat{\epsilon}^{(i)} = \gamma\vec{\mathcal{E}}_i(t_0). \tag{38}$$

This procedure is equivalent to replacing $\vec{\mathcal{E}}(t)$ by $\vec{\mathcal{E}}(t_0)$ in (19) and solving the resulting equation *exactly* for $\vec{p}$. Equation (35) is then satisfied because it follows from the form of Eq. (19) regardless of how $\vec{\mathcal{E}}$ behaves.

Several improvements were also tried. The most important was the use of $\vec{\mathcal{E}}(t_0+\frac{1}{2}\Delta t)$ instead of $\vec{\mathcal{E}}(t_0)$ in Eq. (38). A preliminary value of $\vec{\mathcal{E}}(t_0+\frac{1}{2}\Delta t)$ could be obtained either by extrapolation from the previous step or by interpolation from the approximation to $\vec{p}^{(i)}(t_0+\Delta t)$ given by Eq. (37) with (38) as it stands. The step could then be iterated a few times, each time deriving $\vec{\mathcal{E}}(t_0+\frac{1}{2}\Delta t)$ by interpolation from the result of the previous iteration.

V. NUMERICAL COMPUTATION: RESULTS AND DISCUSSION

A. Mode analysis

With θ initially at any value not too close to $\frac{1}{2}\pi$, the principal prediction of Ref. 8 is clearly confirmed: variations in phase of the dipole density throughout the sample, which at first grow linearly at a rate $\sim T_s^{-1}\Lambda$, presently (in a time $\sim T_s\Lambda^{-3}$) cease to grow and experience a restoring effect. Thereafter, these variations oscillate irregularly in the neighborhood of zero, so that the total dipole moment of the sample remains near its (initial) maximum value for the given θ.

The irregularity is only apparent and comes

from the simultaneous presence of two modes. According to the theory of Ref. 8 as applied to the sphere, there are only two spatial modes directly coupled to the uniform mode (i.e., for which $\xi_\alpha \neq 0$). Their spatial distribution can be expressed as

$$q_1 = a_1\sigma^2 + b_1\zeta^2 + c_1, \qquad q_2 = a_2\sigma^2 + b_2\zeta^2 + c_2, \tag{39}$$

where

$$b_1/a_1 = 3 + \sqrt{\tfrac{15}{2}} = 5.74, \qquad b_2/a_2 = 3 - \sqrt{\tfrac{15}{2}} = 0.261. \tag{40}$$

The corresponding eigenvalues (see Ref. 8) are

$$\eta_1 = -(\tfrac{8}{21}\pi)(1 - 3\sqrt{\tfrac{6}{5}}) = 2.74, \qquad \eta_2 = -(\tfrac{8}{21}\pi)(1 + 3\sqrt{\tfrac{6}{5}}) = -5.13. \tag{41}$$

It follows that the deviations of the local Bloch vector density from its value at the center should behave in space and time as

$$\begin{aligned}|\vec{p}(\sigma,\zeta,t) - \vec{p}(0,0,t)| &= (A_1\sigma^2 + B_1\zeta^2)\Lambda^{-2}\sin\theta\sin(\omega_1 t\, T_s^{-1}\Lambda^3\cos\theta) \\ &\quad + (A_2\sigma^2 + B_2\zeta^2)\Lambda^{-2}\sin\theta\sin(\omega_2 t\, T_s^{-1}\Lambda^3\cos\theta),\end{aligned} \tag{42}$$

where we now take Λ to be precisely $(kR)^{-1}$. The parameters $A_1, B_1, A_2, B_2, \omega_1, \omega_2$ should all be independent of Λ and of θ as long as $\cos\theta$ is not small. The ratios $B_1/A_2, B_2/A_2$ should be the same as $b_1/a_1, b_2/a_2$ in Eq. (40). The size of A_1, A_2 must be such that the initial rate of growth agrees everywhere with the first term of Eqs. (29). The values of ω_1, ω_2 should be

$$\omega_1 = (9/4\pi)|\eta_1| = \tfrac{6}{7}(3\sqrt{\tfrac{6}{5}} - 1) = 1.960, \qquad \omega_2 = (9/4\pi)|\eta_2| = \tfrac{6}{7}(3\sqrt{\tfrac{6}{5}} + 1) = 3.674. \tag{43}$$

To check these predictions, we fitted the *computed* deviations to the formula

$$|\vec{p}(\sigma,\zeta,t) - \vec{p}(0,0,t)| = [A(t)\sigma^2 + B(t)\zeta^2]\Lambda^{-2}\sin\theta \tag{44}$$

at each step in time. Each of the temporal functions A and B was then fitted *independently* to a superposition of two sine waves of arbitrary amplitude and frequency

$$\begin{aligned}A(t) &= A_1\sin(\alpha_1 t\, T_s^{-1}\Lambda^3\cos\theta) + A_2\sin(\alpha_2 t\, T_s^{-1}\Lambda^3\cos\theta), \\ B(t) &= B_1\sin(\beta_1 t\, T_s^{-1}\Lambda^3\cos\theta) + B_2\sin(\beta_2 t\, T_s^{-1}\Lambda^3\cos\theta).\end{aligned} \tag{45}$$

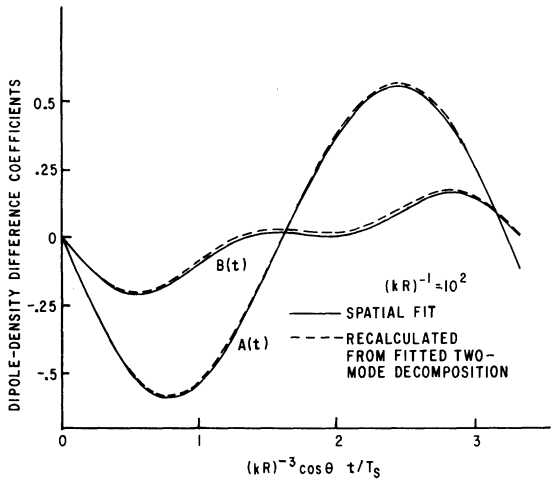

FIG. 2. Time variation of $A(t)$ and $B(t)$, the coefficients of σ^2 and ζ^2 [Eq. (44)] in the computed difference between the dipole density at the center of the sphere and its average throughout the sphere.

The goodness of these fits is shown in Fig. 2.

As shown in Table I, the parameters $A_i, B_i, \alpha_i, \beta_i$ $(i = 1, 2)$ remain nearly constant as predicted over a wide range of values of θ and of $\Lambda = (kR)^{-1}$. Moreover, the prediction $\alpha_1 = \beta_1 = \omega_1$, $\alpha_2 = \beta_2 = \omega_2$ is very well satisfied. The ratios $B_1/A_1, B_2/A_2$ agree to about 10% with those predicted in Eq. (40); we think the discrepancy has to do with the replacement of the spatial continuum by a set of discrete rings. It is well known that a small change in a Hermitian operator affects the eigenfunctions more than it does the eigenvalues.

The oscillations discussed above take place in a time $O[T_s\Lambda^{-3}]$. Therefore the radiative decay of the overall Bloch vector, while present in our

TABLE I. Spatial fitted two-mode decomposition parameters.

$(kR)^{-1}$	θ	α_1	α_2	A_1	A_2	β_1	β_2	B_1	B_2
10	0.1	1.92	3.70	−0.588	−0.0173	1.91	3.69	−0.143	−0.0858
100	0.1	1.94	3.67	−0.580	−0.0182	1.93	3.67	−0.140	−0.0868
100	0.2	1.94	3.67	−0.579	−0.0180	1.93	3.66	−0.140	−0.0866
100	0.6	1.95	3.61	−0.583	−0.0204	1.94	3.65	−0.145	−0.0889
100	1.0	1.95	3.67	−0.581	−0.0201	1.94	3.66	−0.141	−0.0885
100	1.4	1.94	3.68	−0.580	−0.0187	1.93	3.67	−0.141	−0.0872

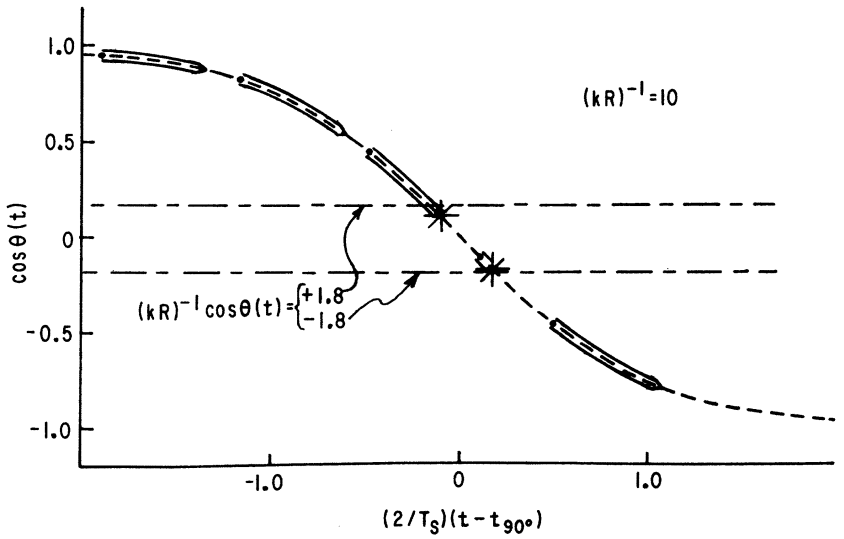

FIG. 3. Time dependence of the average value of the third component of $\vec{p}$ for several initial conditions. Each arrow gives trajectory for a particular computer run whose end points are indicated by the dot at the tail and the arrowhead. The star burst indicates coherence loss. The Dicke decay is shown as a dashed line.

machine computation and detectible in the results, has a negligible effect during a few oscillations. Hence the Bloch angle θ, in all the above equations, is to be understood as the initial value, the error in this replacement being small.

B. Dicke decay

We did, however, run the program for many oscillations with $\Lambda = 10$, so as to follow the system for a time comparable to T_s. We found that the oscillations continued with small amplitude and full coherence was maintained through large changes in θ, as long as we did not pass through the region $\theta \simeq \frac{1}{2}\pi$. We show in Fig. 3 the spatial average of the third component of the Bloch vector as a function of time for various initial conditions corresponding to Eq. (34). We only follow the time evolution of $\langle p_3 \rangle_{av}$ for times of order $(1/4)T_s$. The dashed curve is the Dicke decay obtained from Eq. (1). Each arrow follows the time trajectory of $\langle p_3 \rangle_{av}$ for a particular computer run. The two star bursts replacing the arrow tips indicate the sudden disappearance of the macroscopic dipole moment because of superradiant instability. The time trajectories follow the Dicke decay formula very well.

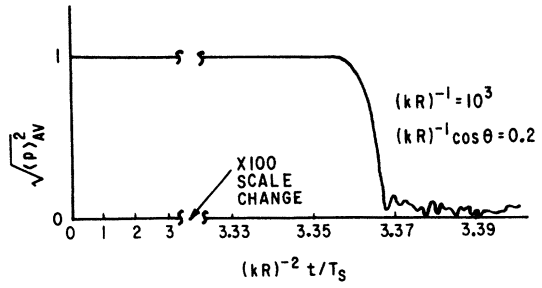

FIG. 4. Time development of $\sqrt{\langle \vec{P} \rangle^2_{av}}$ starting from the coherently excited state $(kR)^{-1}\cos\theta = 0.2$ in the instability region of the Bloch sphere.

C. Equatorial instability

Before discussing our results for $\theta \sim \frac{1}{2}\pi$, we correct some sign misprints in Ref. 8. The sign of $(\eta_\alpha - \eta_0)$ in Eqs. (16) and (17) and η_α in Eqs. (19) and (20) should be reversed. Thus Eq. (20) should read

$$\nu_\alpha^2 = \eta_\alpha^2 \cos^2\theta - \eta_\alpha \xi'_\alpha \sin^2\theta, \tag{46}$$

so that instability is possible when $\eta_\alpha \xi'_\alpha > 0$. The parameters for the unstable mode in the sphere are given correctly, with η_α and ξ'_α both positive. The expression $(kR)^{-1}$ should be replaced by kR on the right-hand side of (22) and (24), but the numerical result of (24) is correct.[21]

For initial values of θ close to $\frac{1}{2}\pi$, the prediction of complete dephasing was dramatically confirmed. A typical plot, showing the root mean square of the magnitude of the *total* Bloch vector as a function in time, is given in Fig. 4. As predicted, the dephasing takes place after a delay $T_\Delta \sim O[\Lambda^{-2} T_s]$ and the duration of the dephasing process is even shorter $O[\Lambda^{-3} T_s]$.

In Fig. 5 we plot the computed values of T_Δ, in units of $T_s \Lambda^{-2}$, against the initial value of $\cos\theta$ in units of Λ^{-1}, for two very different values of Λ. The two sets of points coincide perfectly, as they should according to the theory of Ref. 8.

In the same figure we show the detailed curve expected on the basis of Eqs. (22) and (23) of Ref.

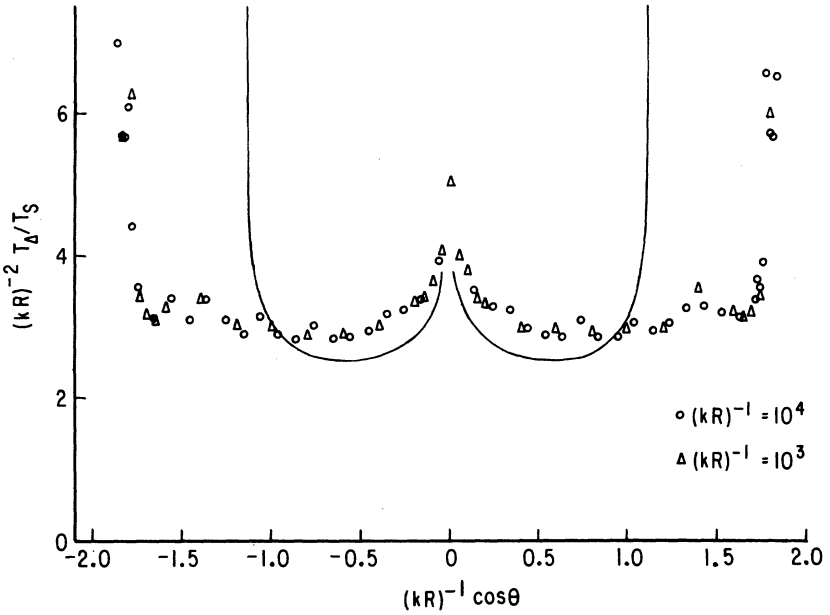

FIG. 5. Threshold time T_Δ in units of $T_s(kR)^2$ for dephasing of the dipole moment density is plotted as a function of $(kR)^{-1}\cos\theta$ for two values of $(kR)^{-1} = \Lambda$.

8. The computed points confirm the shape of the curve, a steep nearly square well with a cusp at the center, and the value of T_Δ in the floor of the well is in good agreement. However, the computation gives the width of the well as about 2× larger than expected from the theory. This means that the first mode appears to be blowing up even at values of $|\cos\theta|$ which according to Eq. (20) of Ref. 8 ought to be large enough to make ν_α^2 slightly positive, ensuring stable oscillations. We think the explanation lies in some combination of mode mixing and nonlinear effects, not yet understood. We note that whereas the data of Fig. 5 shows that superradiant instability sets in once $|(kR)^{-1}\cos\theta| \lesssim 1.8$, the trajectory of Fig. 3 shows that for $(kR)^{-1} = 10$ instability was not macroscopically apparent until $(kR)^{-1}\cos\theta \simeq 1.2$. The reason is that the change in θ due to superradiant damping in the time T_Δ varies as

$$\Delta\theta = (2/T_s)\sin\theta\, T_\Delta \tag{47}$$

from Eq. (1). From Fig. 5 we note that the plateau of T_Δ corresponds to $T_\Delta/T_s \approx 3(kR)^2$ so that (setting $\sin\theta = 1$)

$$\Delta[(kR)^{-1}\cos\theta] \simeq (kR)^{-1}\Delta\theta \simeq 6(kR). \tag{48}$$

For $(kR)^{-1} = 10$, we obtain $(kR)^{-1}\Delta\theta = 0.6$ which is exactly the difference between the values of $(kR)^{-1}\cos\theta$ of 1.8 and 1.2.

VI. CONCLUSION

We have verified by direct computer calculation that superradiance from a coherently excited sphere follows Dicke's equation except in the equatorial region of the Bloch sphere where it suddenly dephases and all coherence is lost. These results obtain for $kR \ll 1$, that is, for sphere of small spatial extent. We have also obtained agreement with the major predictions of Ref. 8 governing the size of the equatorial region of instability and the minimum time it takes to achieve macroscopic dephasing once this region is reached. We note here that for larger spheres we might expect to be able to pass through the equator without complete dephasing. For $kR \simeq 1$ then Eq. (48) gives $(kR)^{-1}\Delta\theta \approx 6$ which is of the order of the extent of the instability region. The approximation associated with kR being small is not very good in this case but it gives rise to an interesting possibility which should be investigated further.

*Work at Columbia supported in part by the Joint Services Electronics Program (U. S. Army, Navy, and Air Force) under Contract No. DAAB07-69-C-0383, and in part by the USAEC.

[1]R. H. Dicke, Phys. Rev. 93, 99 (1954).

[2]N. E. Rehler and J. H. Eberly, Phys. Rev. A 3, 1735 (1971); V. Ernst and P. Stehle, Phys. Rev. 176, 1456 (1968); R. Bonifacio, P. Schwendimann, and F. Haake, Phys. Rev. A 4, 302 (1971).

[3]Even if off-axis radiation can be neglected, as in a long rod, it is never correct, for a mirrorless laser, to ignore Fourier components of slightly off-resonant

wave number.

[4]L. Skribanowitz, I. P. Herman, J. C. MacGillivray, and M. S. Feld, Phys. Rev. Lett. 30, 309 (1973).

[5]V. M. Fain, Zh. Eksp. Teor. Fiz. 36, 798 (1959) [Sov. Phys.—JETP 9, 562 (1959)]; F. T. Arrecchi and D. M. Kim, Opt. Commun. 2, 324 (1970); C. R. Stroud, Jr., J. H. Eberly, W. L. Lama, and L. Mandel, Phys. Rev. A 5, 1094 (1972).

[6]R. Jodoin and L. Mandel, Phys. Rev. A 9, 873 (1974); see also, A. Flusberg, R. Friedberg, and S. R. Hartmann, Phys. Rev. A 10, 1904 (1974).

[7]R. Friedberg, S. R. Hartmann, and J. T. Manassah, Phys. Lett. A 40, 365 (1972).

[8]R. Friedberg and S. R. Hartmann, Opt. Commun. 10, 298 (1974).

[9]For a particular Dicke state the coherent spontaneous emission rate is $I_{\rm coh}=I_0(r+m)(r-m+1)$, whereas $I_{\rm incoh}=I_0(\frac{1}{2}N+m)$. For the largest value of cooperation number $r=\frac{1}{2}N$ this ratio $I_{\rm coh}/I_{\rm incoh}$ is $r-m+1$. For $N\gg 1$ the quantity $r-m+1\gg 1$ for almost all values of m. For example, if $N=2\times 10^5$ then $r-m+1>10$ for $99\,991>m>-10^5$.

[10]M. Planck, Ann. Phys. (Paris) 1, 69 (1900), especially pp. 88–93. In this discussion the resonator is a harmonic oscillator, corresponding to Bloch states very near the "south" (unexcited) pole. The random phase arises in the field instead of in the dipole moment, and the average is taken over the resonator line shape instead of over trials.

[11]We may note that the criterion $I_{\rm coh}\gg I_{\rm incoh}$ does not require that the radiation rate be comparable to N^2I_0. However, it seems likely from Dicke's paper that he intended such a requirement and did not necessarily consider the state ($r=\frac{1}{2}N$, $m=-\frac{1}{2}N+1$), for which $I_{\rm coh}=NI_{\rm incoh}=NI_0$, as superradiant, even though it has the largest possible enhancement factor $I_{\rm coh}/I_{\rm incoh}=N$. The state ($r=\frac{1}{2}N$, $m=0$) for which $I_{\rm coh}=\frac{1}{2}N(\frac{1}{2}N+1)I_0$, $I_{\rm incoh}=\frac{1}{2}NI_0$, has an enhancement factor of only $\frac{1}{2}N+1$.

[12]It has been recently proposed [L. Mandel, R. Jodoin, and J. H. Eberly (private communication)] that the term "superradiance" be reserved for those cases in which radiation reaction cannot be neglected, so that it would not apply to free induction decay or in general to any phenomenon in an optically thin sample. This preference is apparently based on a reluctance to apply a relatively new term "superradiance" to a well-established and independently known phenomenon, free-induction decay. We feel, however, that it is too late, years after Dicke's work, to change the meaning of his terminology. Accordingly we shall say "superradiant reaction" or "superradiant damping" where the aforementioned group would say "superradiance," and we shall consider free induction decay, as well as echo pulses in an optically thin sample, as examples of superradiance (in our sense) without significant superradiant reaction.

[13]R. Friedberg and S. R. Hartmann, Phys. Lett. A 37, 285 (1971).

[14]See Stroud *et al.*, Ref. 5.

[15]E. A. Power and S. Zienau, Philos. Trans. A 251, 427 (1958).

[16]H. A. Lorentz, *Theory of Electrons*, 2nd ed. (Dover, New York, 1952); C. Kittel, Phys. Rev. 73, 155 (1948); R. Friedberg, S. R. Hartmann, and J. T. Manassah, Phys. Rept. 7C, 101 (1973).

[17]M. J. Stephen, J. Chem. Phys. 40, 669 (1964).

[18]A. Szöke and S. Meiboom, Phys. Rev. 113, 585 (1959).

[19]A. Abragam, *The Principles of Nuclear Magnetism* (Clarendon, Oxford, 1961).

[20]This is derived on the assumption that either the dipole moment density is uniform or the dipole placement is cubic and dense.

[21]We note also that in the expression for $G(\vec{s})$ following Eq. (4) of Ref. 8, s^{-3} should be replaced by s^{-5}; and that the left-hand side of Eq. (15) should be $\dot{v}_\alpha$, not v_α.